sciendo

POLISH MARITIME RESEARCH 2 (106) 2020 Vol. 27; pp. 145-157
10.2478/pomr-2020-0036

DESIGN AND MECHANICAL ANALYSIS OF A COMPOSITE T-TYPE CONNECTION STRUCTURE FOR MARINE STRUCTURES

Xiaowen Li
Zhaoyi Zhu
Yan Li
Zhe Hu
Jimei University, School of Marine Engineering, Xiamen, China

ABSTRACT

A new T-type connection structure consisting of composite sandwich plates, reinforced cores and adhesive was proposed for the construction of lightweight ships to resolve connection problems between bulkheads and decks of composite lightweight ship superstructures. Based on the design principles and mechanical properties of composite structures, the mechanical behaviour of the structure under a dangerous loading condition was investigated. In addition, the ultimate bearing capacities and damage modes were examined, the results of which demonstrated that the strength of the structure is weak, and that the adhesive and reinforced core between the face plate and the web plate is the primary weakness of the structure. A numerical simulation method was verified using the results of the mechanical tests, and five characteristic paths at the connection area were established. The stresses and displacements along the five paths were calculated using the numerical method. Then, variations in the geometric parameter and the strength and weight of the connection were summarised. The optimal angle of the adhesive bonding area is approximately 60°, which supports the optimal design and practical application of the lightweight ship adhesive-bonded connection structure.

Keywords: T-type connection structure, composite structure design, test, mechanical analysis, marine structure

INTRODUCTION

Composites are structural-functional materials that have been used in a variety of industries, including the aerospace, automotive, shipbuilding, and chemical processing industries [6, 23]. Due to the ease with which they are mass-produced and their favourable properties, e.g., strength-to-weight ratios, composites are especially utilised for the construction of boats and ships that are less than 100 m long. An observational study found that ships constructed from foam sandwich composites were 36% and 10% lighter than similarly sized steel and aluminium ships, respectively [19].

To enhance the mechanical and physical performances of composite materials, most lightweight composite structures employ adhesive bonding [10], which has been used in manufacturing for more than 50 years [9]. A variety of adhesive bonding forms have been used, including single-lap joints, double-lap joints, docking connections, bevel connections, and trapezoidal connections. Connections represent the primary weaknesses of a structure and have consequently been the focus of many scholars. With the continuous application of composite T-type adhesive-bonded structures in the shipbuilding, aerospace and automobile industries in recent years, the performances of T-type composites have attracted increasing attention from both domestic and foreign researchers [1–5, 7, 12, 15–17, 20–21]. For instance, Diler et al. studied six composite T-type connections comprising sandwich panels and summarised their mechanical properties under tension loads [7]. Toftegaard and Lystrup designed a new T-type adhesive joint composed of sandwich panels and discovered that the lost weight is more valuable by adjusting the design parameters under a certain strength [21]. Shenoi and Hawkins studied the mechanical performance of T-type connections constructed using laminated plates and found

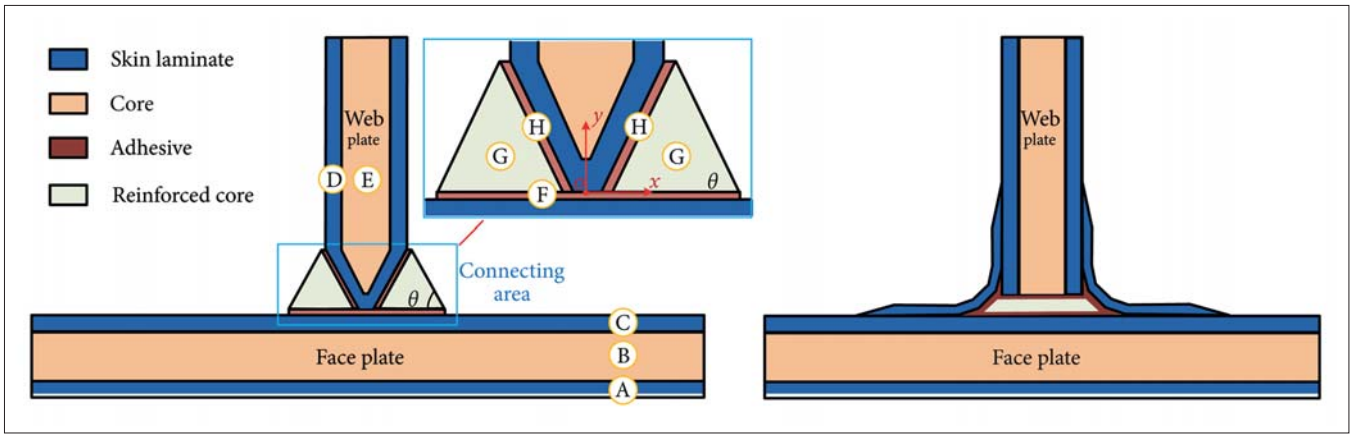

Fig. 1. Scheme for the new T-type composite connection (left) and the traditional design (right)

that both the thickness and the geometrical configuration of the adhesive layer can significantly affect the performance of the connection [16]. Khalili and Ghaznavi investigated the influences of the geometric and material characteristics of T-type connections on their strength and failure modes through numerical analysis [11].

The advantages of T-type connection structures composed of sandwich composites include a flexible design, lighter weight, higher strength capacity and greater reliability. However, the mechanical properties and damage mechanisms of T-type connections are more complicated than those of traditional metal structures. Two research methods are primarily used by domestic and foreign scholars to study the characteristics of such structures: mechanical experimentation and numerical simulation. The primary subjects of current research are variations in the mechanical characteristics of connection structures under different load conditions, various important parameters (e.g., geometric and material properties) that affect connection performance (e.g., mechanical strength and damage mechanisms), and new types of connections. In this paper, a new T-joint consisting of composite sandwich plates, reinforced cores and adhesive is proposed for the connection structures between the bulkheads and decks of composite lightweight ship superstructures. Based on mechanical testing and numerical analysis, the ultimate bearing capacity and characteristic response parameters of the T-joint with respect to its strength and weight were investigated. The mechanical behaviour and damage modes under a dangerous working condition were examined. In addition, the optimal design value, which supports the joint design, lightweight design and practical application of composite ships, was obtained for the response parameters.

DESIGN OF THE COMPOSITE T-TYPE CONNECTION STRUCTURE

An alternative form of a composite connection structure was proposed in this study based on the traditional connection structure used between the deck and the bulkhead or between the bulkhead and the side of the superstructure of a ship. A new T-type composite connection constructed from composite sandwich panels was designed considering its spatial position, geometric shape and material properties, as shown in Fig. 1 (left side). The main difference between the developed T-type connection structure and the traditional structure is that no skin laminates exist outside the reinforced cores. In the present study, our task is to develop a new composite T-joint for lightweight ship superstructures. A traditional design consisting of sandwich panels joined by adhesive and laminates has been proposed by foreign scholars [21] and is shown in Fig. 1 (right side). Various improved T-joints have been designed and investigated [21]. Some scholars have focused on improving strength (with laminate), while others have focused on reducing weight (without laminate) [8, 18, 22]; this article focuses on the latter. The present design without laminate represents a T-type connection, which has less weight and appropriate strength. Furthermore, this paper indicates that a T-type connection is a weak bearing structure used in superstructures and does not participate in the total longitudinal bending.

The proposed composite T-type connection is constructed during a bonding process using the deck as a web plate and the bulkhead as a face plate. The structure is divided into three components: the face plate (see ○A, ○B, and ○C in Fig. 1), the web plate (see ○D and ○E in Fig. 1) and the connecting area (see ○F, ○G, and ○H in Fig. 1), which includes skin laminate (○A, ○C, and ○D), a core (○B and ○E), adhesive (○F and ○H) and a reinforced core (○G). The skin laminate is composed of fibre-reinforced plastic (glass fibre-reinforced polymer (GFRP) or CFRP), and the core and reinforced core are composed of ship foam. A stronger material can be selected for the reinforced core to increase the strength of the T-type connection structure, and the adhesive is a suitable resin for ships. The T-type connection consists of 8 parts produced by the hand-lay-up process.

The innovation of the composite T-type connection is represented by the detailed design of the connecting area. A continuous, uninterrupted V-shaped skin was proposed for the web plate. The skin of the web plate and the core of the connecting area are bonded together directly, which is different from a previous design (a web plate-adhesive-reinforced core). The new GFRP design (i.e., a skin laminate ○, D-adhesive ○, H-reinforced core ○, G-reinforced core ○, F) includes a protective

Tab. 1. Geometry variables for the composite T-type connection structure

Variable	Unit	Reference value	Description
La	(mm)	350	Length of the core for the face plate
Lb	(mm)	153.5	Length of the core for the web plate
Ta	(mm)	35	Thickness of the core for the face plate
Tb	(mm)	34	Thickness of the core for the web plate
Tma	(mm)	2.4	Thickness of the skin for the face plate
Tmb	(mm)	2	Thickness of the skin for the web plate
Lo	(mm)	5	Minimum core thickness for the web plate
Tj	(mm)	3	Thickness of the adhesive
θ	(°)	60	Angle of the reinforced core
W	(mm)	100	Overall width of the T-type connection

function for the cores of the face and web plates; thus, since the overall weight and cost of the composite connection structure are reduced, lower-density core materials are optional.

The geometric dimensions are shown in Fig. 2, and the meaning of each symbol is given in Table 1 together with a reference value for the initial proposed configuration. The coordinate system in Fig. 2 shows the x- and y-directions along the face plate and the web plate, respectively.

Due to the location and role of the T-type connection structure within the structure of a ship, the connection between the deck and the bulkhead of the lightweight superstructure is dominated by vertical forces. Considering its geometric characteristics, the T-type connection structure has the strongest ability to withstand compression, followed by tensile strength, and its ability to withstand shear stress is the weakest [13]. Therefore, when the proposed composite T-type connection is used as a marine connection structure, the force characteristics of the specific position should be a primary consideration. In addition, according to the strength requirements of the T-type connection under different load conditions and the main structure of the T-type connection, the composite T-type connection can be expanded and strengthened to meet practical requirements for ship design and structural strength needs. Therefore, this condition was designed to investigate the mechanical properties of the T-type connection and to judge its applicability as a marine connection structure. Fig. 3 shows the boundary conditions applied to a T-type connection structure, where *P* and *D* represent the force and constrained distance, respectively.

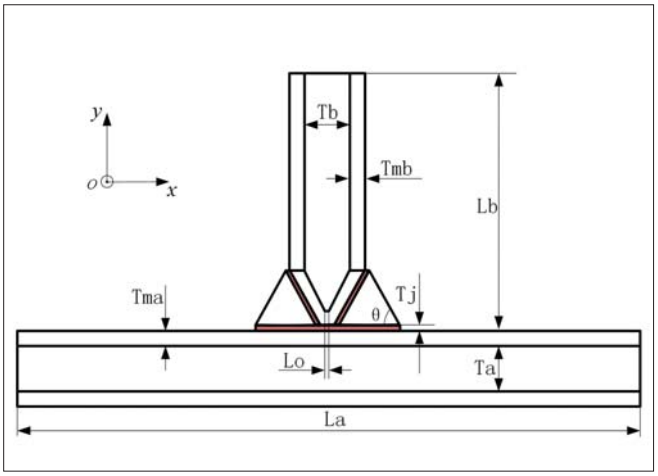

Fig. 2. Geometric dimensions of the proposed composite T-type connection

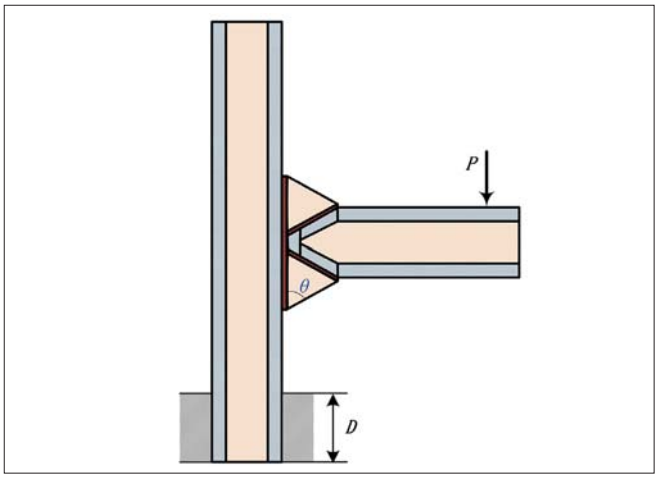

Fig. 3. Loading condition of the composite T-type connection structure

MECHANICAL TESTS AND NUMERICAL SIMULATIONS

MATERIALS AND SPECIMENS

The main component of the proposed composite T-type connection is the sandwich structure, and the primary formation method is the bonding process. The composite sandwich structure has a special form: the outside includes two thin skins, and the inner structure is a single thick core. The outside skin is subjected to tensile and compressive stresses, while the local bending stiffness is small and can be considered negligible. FRP was selected to meet the requirements of the anisotropic mechanical properties, design freedom and the desired surface treatment. The purpose of the sandwich structure core is to support the

skin such that neither inward nor outward deformation is produced during loading and to maintain the skins in their appropriate positions. Low-density foam and balsawood were selected as cores. The composite T-type connection structure proposed in this study was designed for the superstructure of a ship. In addition to considering various mechanical properties, including the strength, stiffness and fatigue, the physical properties of the material itself are considered, such as corrosion and fire resistance and insulation. Due to its numerous advantageous properties, including its light weight, high strength, corrosion resistance and temperature and noise insulation, an E-glass woven roving fabric (EWR200, with a single-layer thickness of 0.4 mm) was selected for the skin material of the sandwich structure. MYcell MC080 structural foam, which is a closed-cell cross-linked polymer with a high strength/stiffness-weight ratio, low resin absorption, high impact and fatigue resistance, weak water absorption and high corrosion resistance with self-extinguishing noise and heat insulation, was selected for the core material of the sandwich structure. In addition, this particular core material, which is suitable for hand pasting/spraying, vacuum import, bonding, pre-impregnation and other moulding processes, is most commonly used as a lightweight core material for structures under static and dynamic loads. A high-performance methyl ethyl ketone peroxide (MEKP)-cured (2% w/v) polyurethane acrylic structural adhesive (Crystic Crestomer 1152PA) was selected for the bonding material, which has been certified by the Italian classification society RINA and is suitable for the bonding of GRP structures.

A 1/2-scale composite T-type connection specimen (shown in Fig. 4) was produced via hand lay-up moulding. The E-glass fibre cloth and resin combined with a curing agent were manually laid out in layers. The mould, which was coated with a release agent, was dripped onto the final layer to form a coat, and then the bubbles were removed. Laminating was performed to the specified thickness, followed by curing to form the specimen. Fig. 5 shows the construction process of the composite T-type connection specimen. The 8 parts were

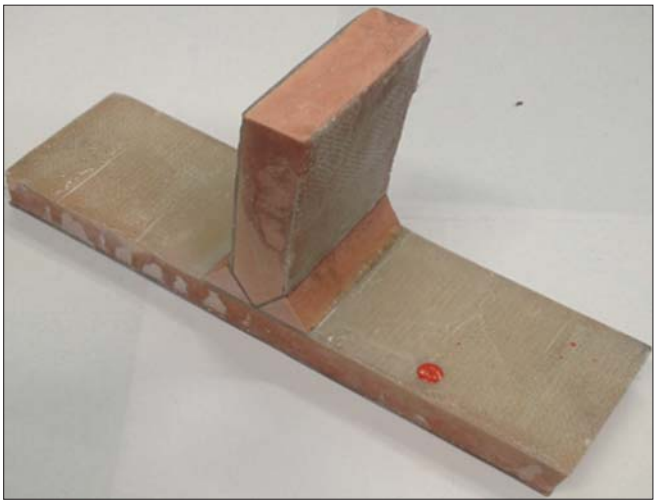

Fig. 4. Composite T-type connection specimen

incorporated into the desired T-type connection specimen through a 9-step hand lay-up process. Three specimens were prepared according to the test conditions.

TESTS AND RESULTS

No definitive reference standard is currently available for mechanical performance testing of T-type connection structures composed of composite sandwich material. Therefore, a test scheme was designed according to the traditional test flow and application environment for a T-type connection structure. Fig. 6 shows the test performed on the specimens. Due to the special form of the proposed T-type connection structure, a special slot clamp was used to fix the face plate. The constrained distance D was 50 mm. A computer-controlled electronic universal testing machine (WDW3100) was used to apply a continuous displacement load to the side of the web plate (20 mm from the end) until the final failure of the specimen was reached. The loading rate was 0.2 mm/min.

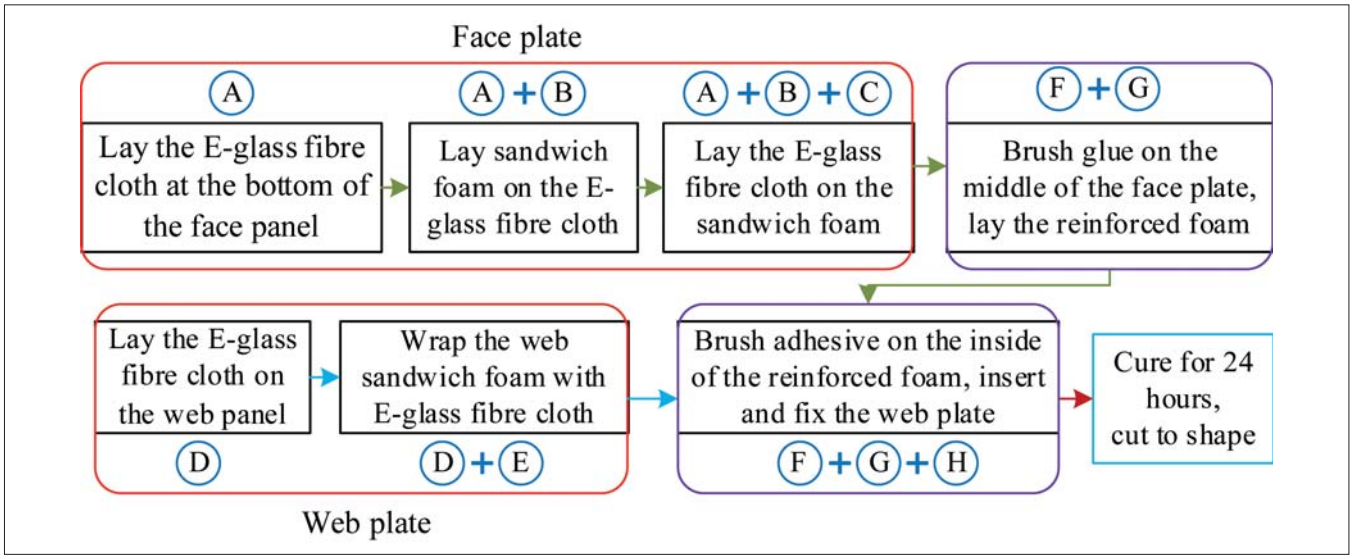

Fig. 5. The hand lay-up process to construct the composite T-type connection specimen

Fig. 6. Mechanical test for the T-type connection specimens

The load versus displacement curves are illustrated in Fig. 7, and the results demonstrate good consistency. At the initial stage of loading, the force and displacement were linearly related to a bending stiffness of approximately 0.125 kN/mm. With an increasing load, the three curves exhibited small fluctuations at P ≈ 0.24 kN, representing the initial failures of the specimens with a slight decrease in the overall stiffness. The specimens still had high carrying capacities, indicating that the failure zone was small. The load was continuously applied until the failure area suddenly expanded, and the failure propagated through the adhesive interface between the web plate and the upper reinforced core after the crack extending to the lower reinforced core of the specimen collapsed completely. Therefore, the ultimate loads of the three specimens were 1.35 kN, 1.36 kN and 1.38 kN.

The reason for this phenomenon is that the top of the web plate was subjected to a concentrated force, which was transmitted along the web plate and through the connection area. With increasing displacement at the top of the web

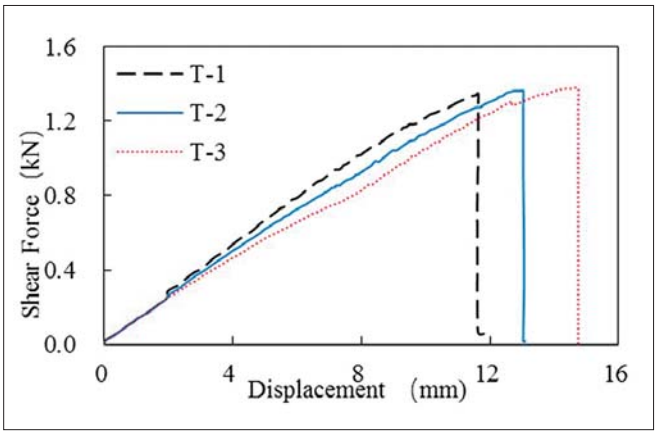

Fig. 7. Load versus displacement curves of the specimens

plate, the web plate exhibited a cantilever bending state, and the face plate was subjected to a bending moment. At this time, in the connection area, shear stress and normal stress at the reinforced core–skin laminate interface will develop to balance the concentrated load and clockwise bending moment at the top of the web plate. When this shear stress and normal stress reached the bonding strength and shear strength at the interface, respectively, a stripping phenomenon occurred and then gradually expanded.

Because the failure processes of the three test specimens were similar, one specimen was selected for illustrative purposes. Corresponding to the failure modes shown in Fig. 8, the initial failure occurred at the connecting area near the web plate (i.e., the position in the white solid circle), and peeling occurred at the area between the upper reinforced core (part ○G) and the upper adhesive (part ○H). With increasing displacement, the damage continued to expand, and when the lower reinforced core cracked along a direction 30° to the normal direction of the face plate, structural collapse occurred. The failure process can be divided into the following three stages: initial failure, cracking and expansion, and final failure, as shown in Fig. 8.

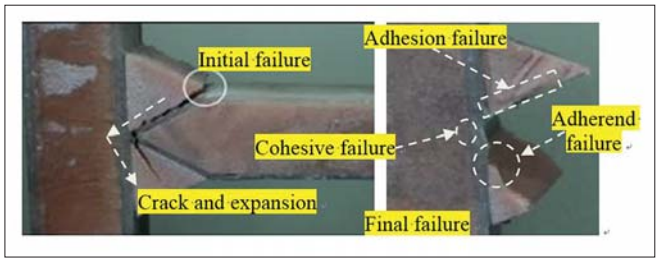

Fig. 8. Failure modes of the tested specimen

Since the time between initial failure and final peeling is very short, the initial failure point and the path of crack propagation during the test are difficult to observe directly. The damage pattern of the specimens is complicated and includes cohesive failure, adhesion failure and adherend failure (see Fig. 8).

The mechanical curves and ultimate loads of the three specimens are fundamentally similar, indicating that the production process of the specimens was relatively stable. In this paper, a mean value of 1.36 kN was selected as the ultimate load of the composite T-type connection with a local shear strength (σ_s) of 0.07 MPa; $\sigma_s = P/A$, where P and A represent the applied load and the area between the connection area and the panel, respectively.

NUMERICAL SIMULATIONS

To save time and improve efficiency, an effective numerical simulation was employed to predict the ultimate bearing capacity of the new T-type connection. Based on the test results, a numerical analysis of the T-type connection specimen under the same condition was conducted using the common finite element calculation platform Ansys19.0 (ANSYS Inc.). To simplify the calculations and improve the operational efficiency, a two-dimensional model (see Fig. 9) was established within a Cartesian coordinate system. The structural characteristics of the skin laminate, core and adhesive layer were simulated using

Tab. 2 Material properties of each component in the composite T-type connection structure

Part	Material	Coordinate system	E_x (MPa)	E_y (MPa)	G_{xy} (MPa)	ν_{xy}	X (MPa)	Y (MPa)	S (MPa)
Skin	GRP	Global	72000	72000	29800	0.21	240	120	200
Skin	GRP	Local	72000	72000	29800	0.21	240	120	200
Core	MC080	Global	104	104	30	0.35	1.45	1.45	1.2
Core	MC080	Local	104	104	30	0.35	1.45	1.45	1.2
Adhesive	1152PA	Global	500	500	170	0.47	15	15	8.7

the structural element PLANE183 with a 2x2 Gauss integration scheme. PLANE183 is a higher-order 2-D, 8-node element with quadratic displacement behaviour and is well suited for modelling irregular meshes. Each node has two degrees of freedom: translations in the nodal x and y directions. The element can be used as a plane element (plane stress, plane strain and generalised plane strain) or as an axisymmetric element. The characteristics of the contact surface between the skin laminate, core and adhesive layer were simulated using the cohesive force models targe169 and conta171. ANSYS supports rigid and flexible body surface-to-surface contact elements, where the rigid surface is regarded as the target, targe169 is used to simulate the 2-D target surface, and the surface of the flexible body is used as a contact by conta171. The numbers of elements and nodes in this model are 30378 and 92157, respectively. Fig. 2 shows the dimensions of the structure, and Fig. 3 demonstrates the loading condition. In addition, Table 2 displays the material properties of the different components (see [12]).

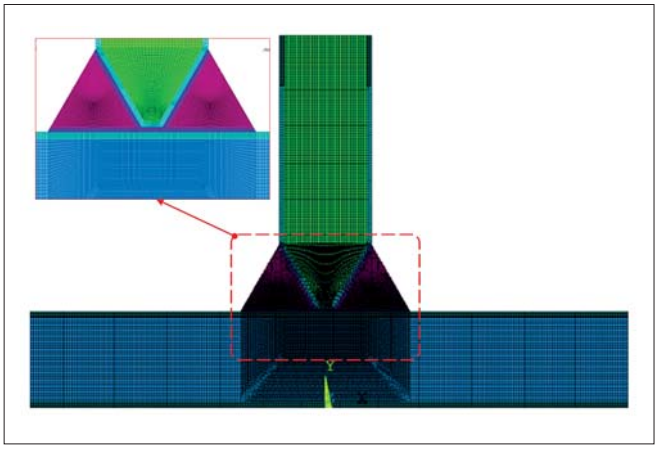

Fig. 9. Two-dimensional model of the composite T-type connection

The Hoffman criterion (see formula (1)) and the maximum stress criterion (see formula (2)) were used to simulate the failure of the skin laminate, core and adhesive layer [13, 14]. The Hoffman criterion considers the effects of materials with different tensile and compressive strengths on structure failure and adds the two odd function terms (σ_1 and σ_2) on the basis of the Tsai-Hill criterion. Based on [14], the Hoffman criterion was used to evaluate the failure of the skin laminate. The adhesive layer is an important part of the bonding structure and serves as the connecting link between the composite skin laminate and the core. According to the experimental study, the mechanical properties of cured resin are similar to those of a brittle material; therefore, the resin can be regarded as a linear elastic material. Based on [13], the maximum stress criterion was used to evaluate the failure of the adhesive layer. The foam material is nearly quasi-isotropic, and the core material in this article is MC080. The test shows that MC080 has a certain brittleness; therefore, the maximum stress criterion was also used to determine whether the core material fails.

$$F_{11}\sigma_{11}^2+2F_{12}\sigma_{11}\sigma_{22}+F_{12}\sigma_{22}^2+F_{66}\sigma_{66}^2+F_1\sigma_{11}+F_2\sigma_{22}=1$$

$$F_1=\frac{1}{X_T}-\frac{1}{X_C},\ F_2=\frac{1}{Y_T}-\frac{1}{Y_C},\ F_{11}=\frac{1}{X_T X_C},\ F_{12}=-\frac{1}{2X_T X_C},$$

$$F_{22}=\frac{1}{Y_T Y_C},\ F_{66}=\frac{1}{S^2}, \tag{1}$$

$$\sigma_{11}=X_t,\ \sigma_{22}=X_t,\ |\tau_{12}|=S \text{ or } |\sigma_{11}|=X_c,\ |\sigma_{22}|=Y_c,\ |\tau_{12}|=S \tag{2}$$

A stiffness reduction process was carried out using a complete attenuation moment unloading model. The Newton–Raphson method with a tangent stiffness matrix and a load step was used to obtain the nonlinear solution. In summary, the numerical simulation of the composite T-type connection was designed to calculate the ultimate carrying capacity, as shown in Fig. 10.

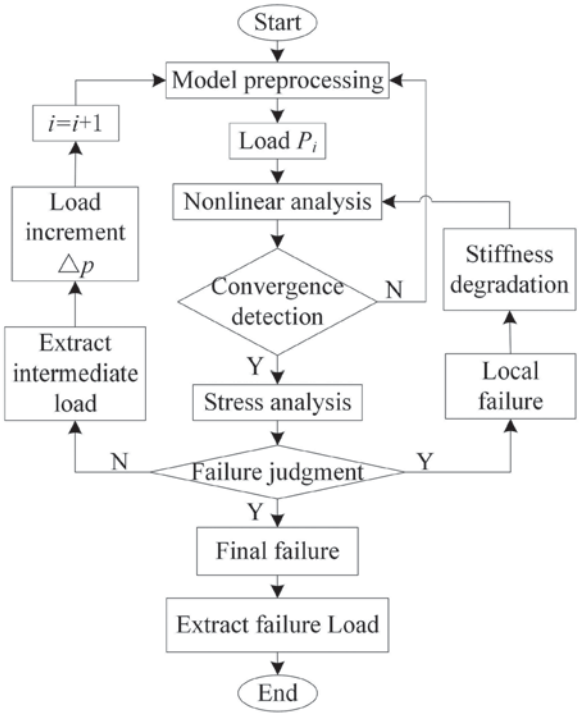

Fig. 10. Numerical simulation algorithm

The results of the mechanical tests demonstrate that the load versus displacement curves of the specimens exhibit good consistency, with similar ultimate load and stable formation processes. Therefore, an approximate mean curve of T-1, T-2 and T-3 from the experiments was selected as the criterion for the numerical simulation. Fig. 11 shows that the simulated (FE) and approximate mean (test) curves are essentially similar in this scenario. The initial failure and the maximum load obtained through the numerical method (the FE curve) are 0.251 kN and 1.388 kN, respectively, with errors of 4.6% and 2.2%, respectively, compared with the test values. Therefore, the above results prove the validity of the numerical method for analysing the strength of the composite T-type connection and provide theoretical support for follow-up research on the corresponding response parameters.

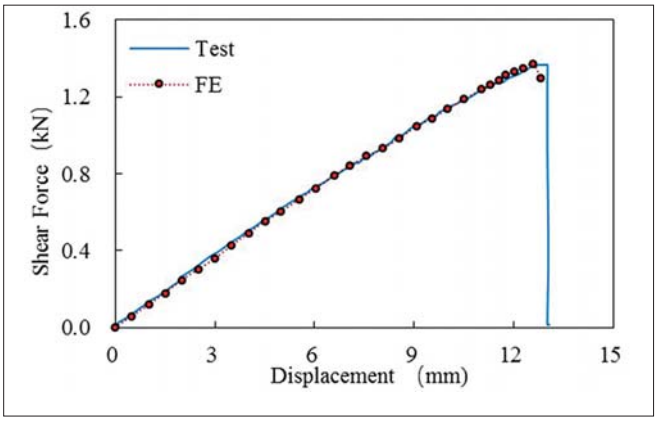

Fig. 11. Comparison of the test result and FE calculation

RESPONSE PARAMETERS FOR THE STRENGTH AND WEIGHT

The experimental results reveal that the strength of the composite T-type connection is weak, that the bonding position between the core of the connection area and the web face is the primary source of weakness, and that the damage mode of the adhesive material is complicated. Based on the numerical simulation conducted in the numerical simulations section above, the mechanical properties of the composite T-type connection structure under the same loading condition were studied. The stress characteristics and the structural weight were investigated, the details of which are shown in Fig. 12.

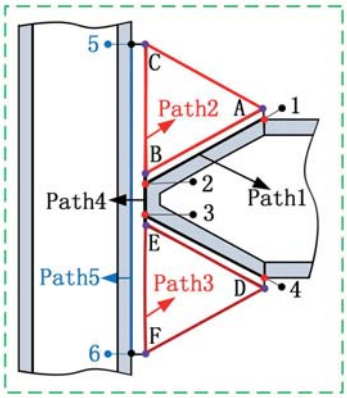

Fig. 12. Characteristic paths of the composite T-type connection

For T-type connections, the geometry of the reinforced core is directly related to the geometry of the adhesive layer, which has an important effect on the connection strength. Five characteristic paths were established (path 1: 1-2-3-4, path 2: A-B-C, path 3: D-E-F, path 4: B-E, and path 5: 5-6), as shown in Fig. 12. The influence of the geometric parameter on the mechanical properties and weight of the connecting structure was analysed with respect to variations in angle θ. Angle θ changed from 15° to 75° with an interval of 15°. Fig. 13 shows the geometries corresponding to different angles. In addition, the optimal angle θ was obtained to guide the design and optimisation of the connection structure. When selecting the optimal angle, the minimum weight was taken as the objective function, and the stress and displacement on the 5 paths were taken as the constraint conditions.

The stress and displacement curves of the adhesive layer along path 1 were calculated through numerical simulation, as shown in Fig. 14. Since path 1 is geometrically symmetric and the force is asymmetric, its stresses are asymmetrical, while the total displacement is approximately asymmetric. First, we analysed the displacement characteristics. The trend of the total displacement was the same regardless of the value of θ; the maximum values were observed at the left end (Point 1) of the path, and the displacement decreased smoothly towards the middle. When θ increased from 15° to 60°, the corresponding value of the total displacement at the end increased sharply; however, when θ continued to increase, no significant effect on the total displacement was observed. Second, we analysed the stress characteristics. The trend of the stress relative to different values of θ was consistent and smooth except for regions of mutation at the ends and middle of the path. The ends (point 1 and point 4) of path 1 are free ends representing the junctions of different materials, leading to concentration of the stresses. Local stress fluctuations were observed in the centres of the paths (point 2 and point 3) due to the existence of geometric mutations and the criticality of the PVC cores. Variations in θ (15° to 60°) exhibited a different influence on the stresses of path 1. In the region between point 2 and point 3, changes in θ had no effect on stresses. In other regions, the normal stress in the x-direction and the shear stress decreased with an increasing value of θ, while the normal stress in the y-direction increased with an increasing value of θ. In summary, the optimal value of θ is 60° considering the stresses and displacement of path 1 alone.

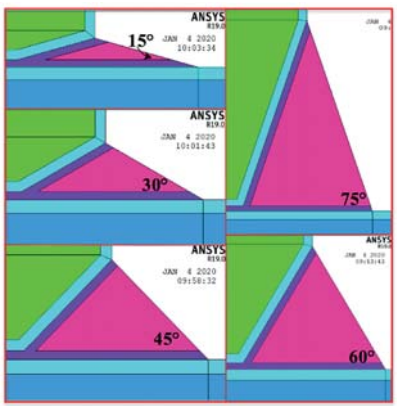

Fig. 13. Geometries with different angles of the connection area (half)

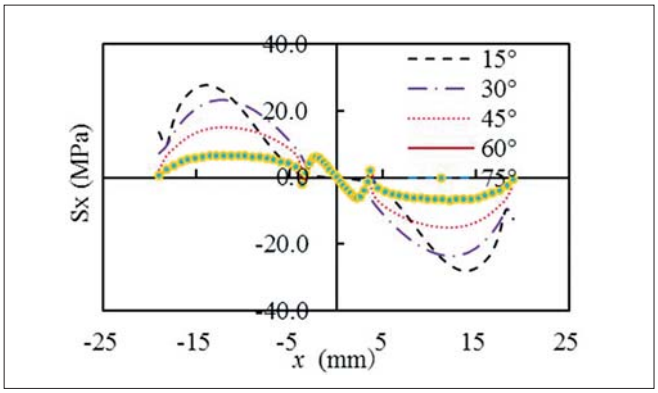

(a) σx

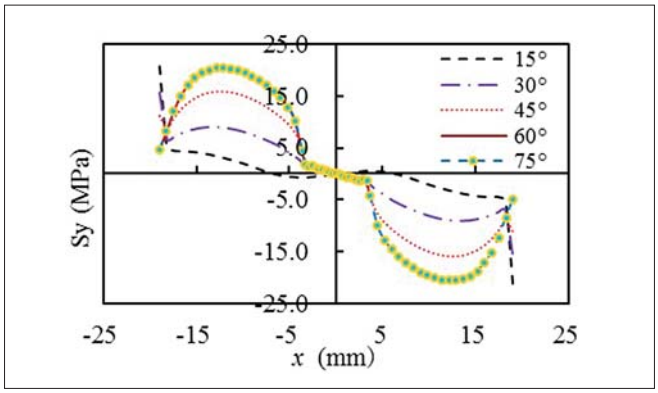

(b) σy

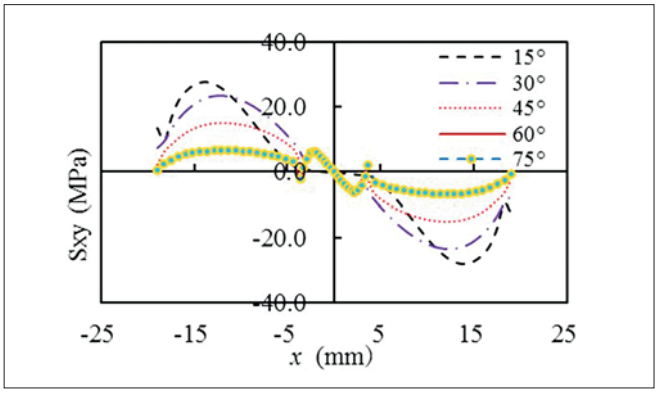

(c) σxy

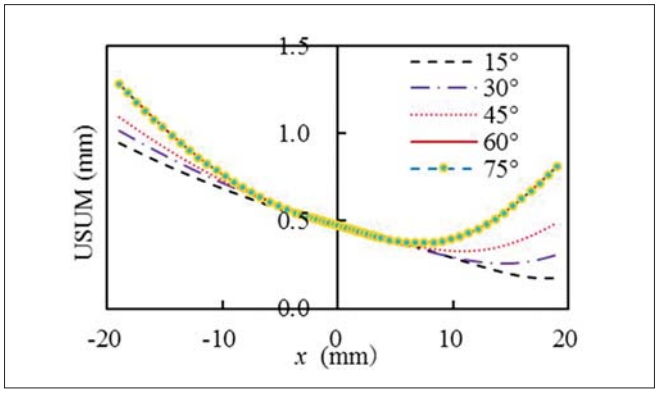

(d) Total displacement

Fig. 14. Stress and displacement curves for path 1 at different angles

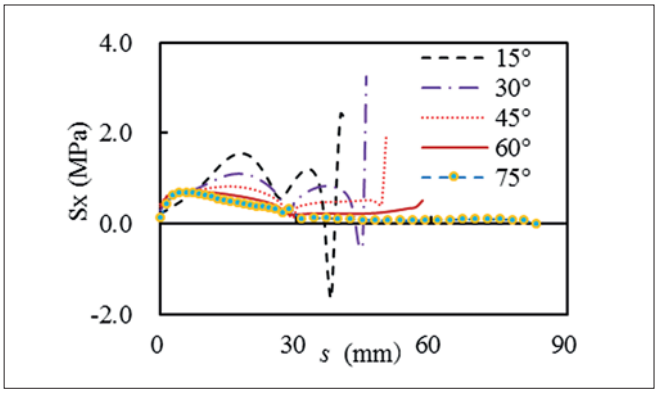

(a) σx

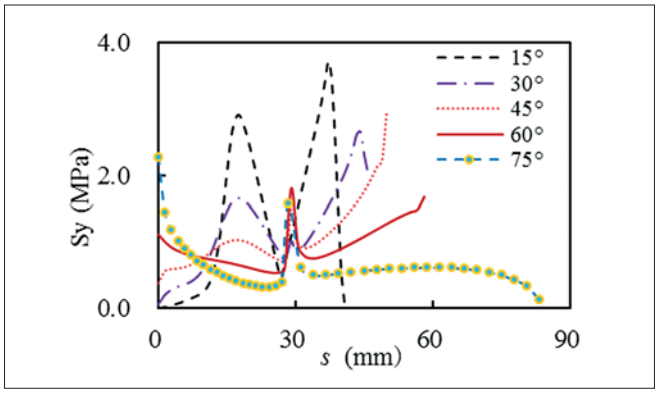

(b) σy

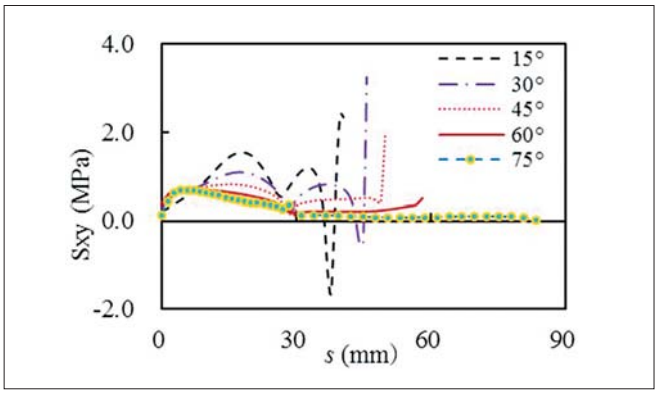

(c) σxy

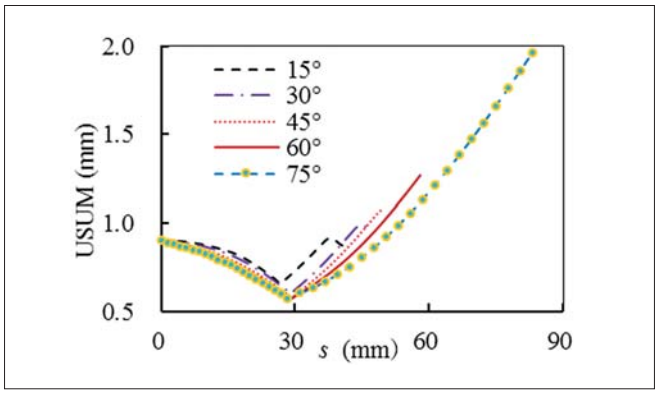

(d) Total displacement

Fig. 15. Stress and displacement curves for path 2 at different angles

The calculation results for path 2 are shown in Fig. 15. The trends of the total displacement relative to different values of θ were the same, with the displacement decreasing with an increasing θ. Because of the geometrical mutation at point B, the displacement curve showed a mutation at point B. Smaller angles produced more obvious downward trends in the displacement. Meanwhile, the trends of the stresses relative to different values of θ were basically the same, with the stress values decreasing with an increasing θ, but different phenomena were detected at the ends of paths A and C and at the centre of path B due to end effects and material mutations. When θ increased from 15° to 45°, the stress value changed abruptly, and obvious concentrations of stress were noted at points B and C. When the value of θ was either 60° or 75°, the normal stress in the x-direction and the shear stress distribution tended to be gentler except for a stress peak at point B. In addition, the trend of the normal stress in the y-direction differed from the others, especially at point A, with the stress increasing with an increasing value of θ. Therefore, the optimal value of θ is 75° considering the stresses and total displacement along path 2.

The calculation results for path 3 are shown in Fig. 16. Since path 2 and path 3 are geometrically symmetric, their stress and displacement curves are fairly similar, especially the stress curves. The trends of the stresses relative to different values of θ were basically the same, with the stress values decreasing with an increasing θ, but different phenomena were detected at the ends of paths D and F and at the centre of path E due to end effects and material mutations. When θ increased from 15° to 45°, the stress value changed abruptly, and obvious concentrations of stress were noted at points E and F. When the value of θ was either 60° or 75°, the normal stress in the x-direction and the shear stress distribution tended to be gentler except for a stress peak at point E. In addition, the trend of the normal stress in the y-direction differed from the others, especially at point D, with the stress increasing with an increasing value of θ. Meanwhile, the trends of the total displacement relative to different values of θ were the same, with the displacement increasing with an increasing θ. Because of the geometrical mutation at point E, the displacement curve showed a mutation at point E. Smaller angles produced more obvious upward trends in the displacement. Therefore, the optimal value of θ is 60° considering the stresses and displacement along path 3.

Path 4 is geometrically symmetric, and the force is asymmetrical; thus, the displacements and stresses are symmetrical, and the shear stresses are asymmetric. Fig. 17 shows the calculation results for path 4, which demonstrate that the displacement and stress changes were consistent for different angles. The total displacement decreased sharply from the left end to the right end, and the displacement value did not substantially change with an increasing θ. Relative to displacement, the stress fluctuations along path 4 were more obvious; larger angles produced higher normal stress values in the y-direction and more active mutations. Stress peaks were detected near point 2 and point 3. The normal stress in the x-direction and the shear stress exhibited different trends,

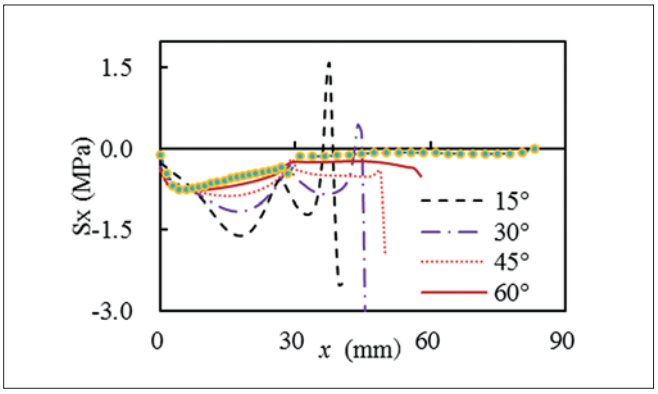

(a) σx

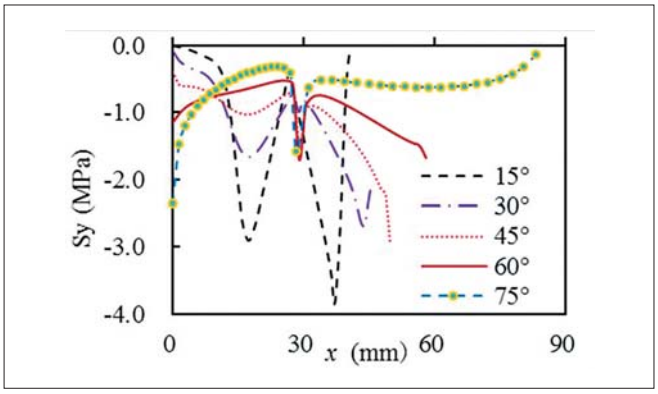

(b) σy

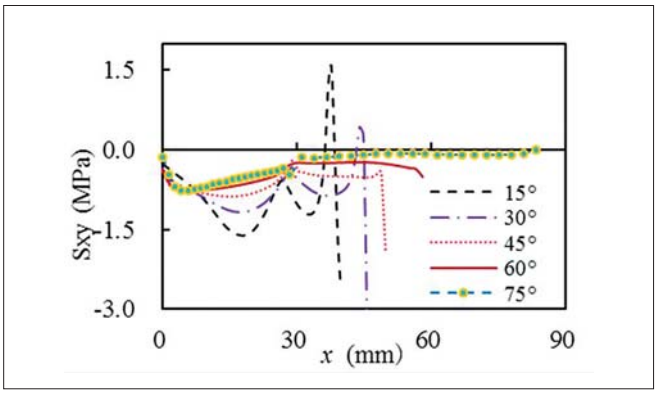

(c) σxy

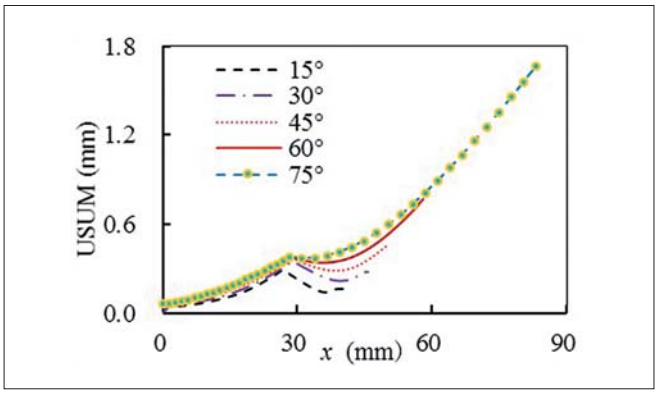

(d) Total displacement

Fig. 16. Stress and displacement curves for path 3 at different angles

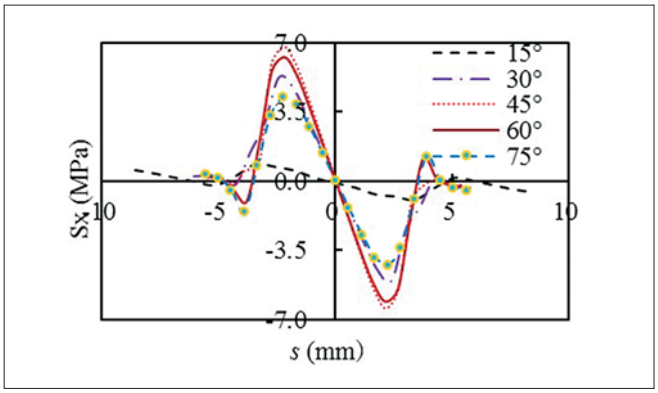

(a) σx

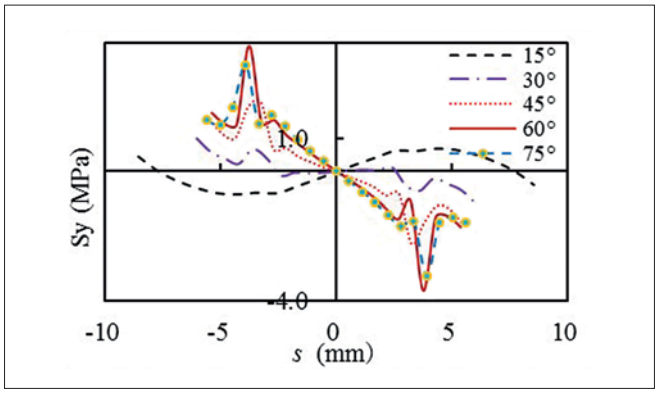

(b) σy

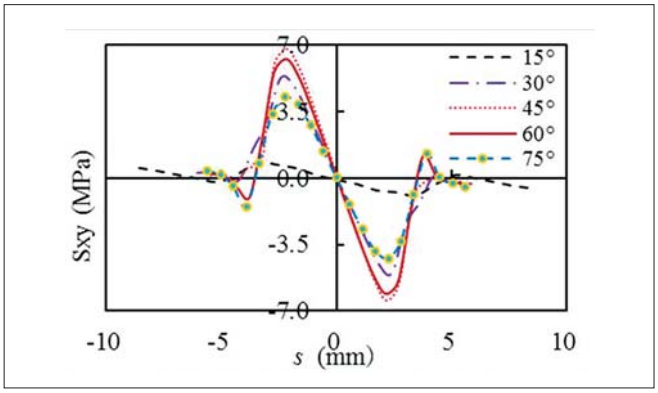

(c) σxy

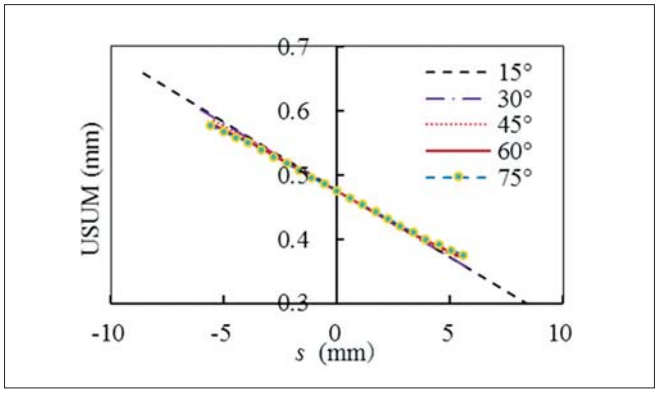

(d) Total displacement

Fig. 17. Stress and displacement curves for path 4 at different angles

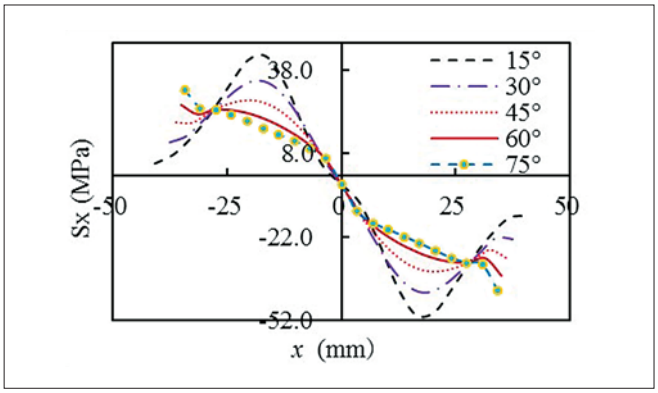

(a) σx

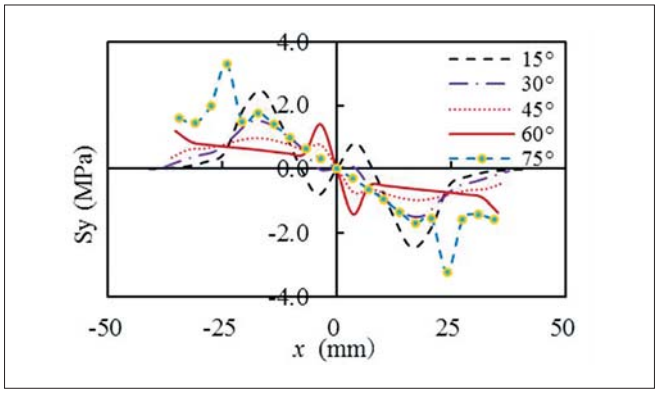

(b) σy

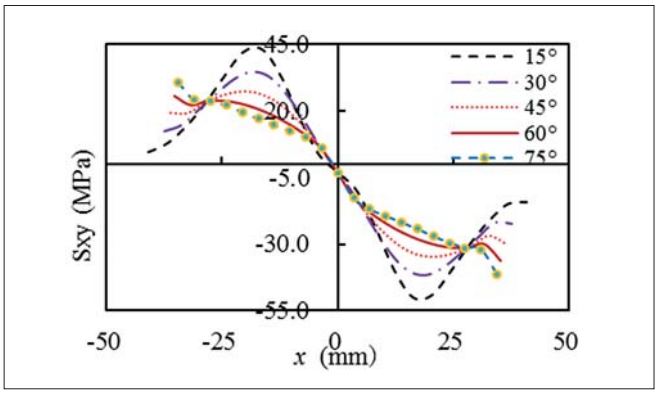

(c) σxy

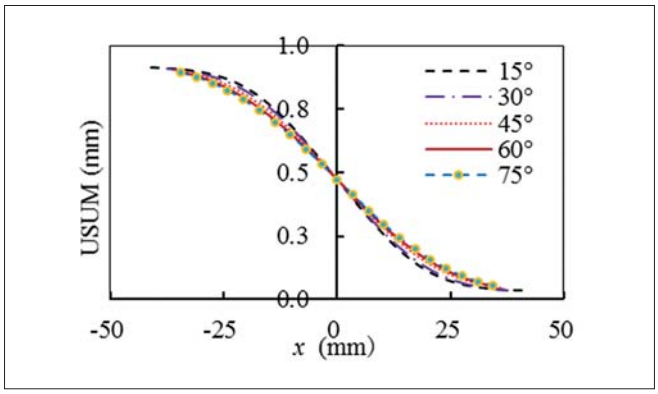

(d) Total displacement

Fig. 18. Stress and displacement curves for path 5 at different angles

with the stress initially increasing and then decreasing as θ increased. The curve at 45° showed large mutations at point 2 and point 3. In summary, the optimal value of θ is less than 45° or greater than 60° considering the stresses and total displacement along path 4.

Path 5 and path 4 are fairly similar but have different geometric positions. The displacements and stresses along path 5 are asymmetrical. Fig. 18 shows the calculation results for path 5, which demonstrate that the displacement and stress changes were consistent for different angles, except for the normal stress in the y-direction. The total displacement decreased rapidly from the left end to the right end, and the displacement value decreased slightly with an increasing θ. The stress fluctuations along path 5 were more obvious; larger angles produced higher normal stress values in the y-direction and more active mutations. Stress peaks were detected near point 5 and point 6. The normal stress in the x-direction and the shear stress exhibited different trends, with the stress decreasing when θ increased from 15° to 75°. The curves between 45° and 75° displayed large mutations near the ends. In summary, the optimal value of θ is greater than 45° considering the stresses and total displacement along path 5.

The above five pictures are similar and emphasise the stress and displacement characteristics of the connection area under different paths and the influence of changes in the geometric parameter (angle θ) on the mechanical properties. The length and position of path 4 are fixed and do not change with angle θ. The stresses and displacement on different paths are the constraint conditions used to identify the lightweight connection structure or the optimal angle. In the process of selecting the optimal angle, a large stress concentration and displacement fluctuations are undesirable. In summary, 60° may be the optimal angle to satisfy the constraints.

The weights of the composite T-type connection at different angles were calculated, as shown in Fig. 19. The minimum weight was observed when the value of θ was 60°, and the maximum weight was 0.727 kg, which corresponded to an angle of 75°. Considering the displacement, stresses and weight of the composite T-type connection, the optimal value of θ should be approximately 60°. Based on specific weight and strength requirements, however, the value of θ can be adjusted accordingly.

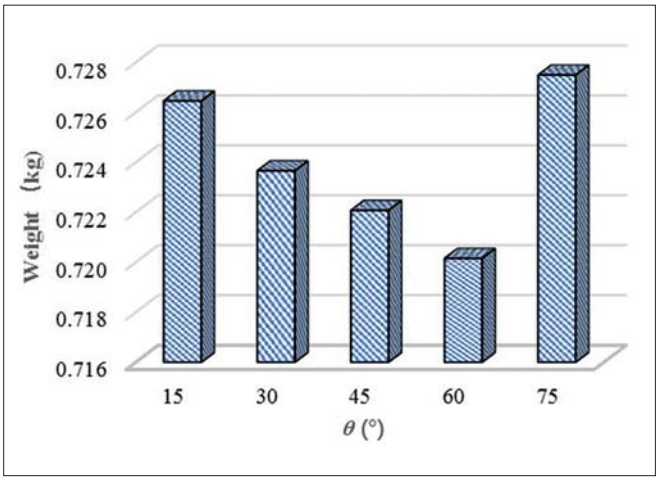

Fig. 19. Weights of the composite T-type connection at different angles

CONCLUSIONS

In this paper, a new T-type connection structure composed of composite sandwich panels and triangular PVC cores was designed to resolve connection problems between the bulkheads and decks of composite lightweight ship superstructures. Because the T-type connection structure is a weak bearing structure in the superstructure and does not participate in the total longitudinal bending, we designed this T-type connection without laminates outside the reinforced cores to reduce the weight. Based on mechanical tests, the ultimate bearing capacity of this composite T-type adhesive connection was examined, and the results revealed that the damage mode of the adhesive is complex, and that the ability of the T-type connection to withstand this dangerous load is weak. Under this loading condition, the initial failure occurred at the connecting area near the web plate, and peeling occurred at the area between the upper reinforced core and the upper adhesive. The connection area experienced cohesive failure, adhesion failure and adherend failure simultaneously. The numerical simulation verified that using the results of mechanical tests is important for determining the strength properties of this T-type connection. Based on the FE analysis, the influences of the geometric parameter of the connection area on the strength and weight of this T-type connection were investigated. Considering the minimum weight and strength constraints of this T-type connection, the optimal value of the geometric response parameter (i.e., angle θ) is approximately 60°. This paper therefore provides a reference for the design and analysis of a composite T-type bonded connection structure for marine composites.

ACKNOWLEDGEMENTS

This work was financed by the National Natural Science Foundation of China (Grant No. 51909103) and the Natural Science Foundation of Fujian Province of China (Grant No. 2018J05090).

REFERENCES

1. Alfano G., Crisfield M. A. (2001): *Finite element interface models for the delamination analysis of laminated composites: mechanical and computational issues*. International Journal for Numerical Methods in Engineering, Vol. 50(7), 1701–1736.

2. Bella G. D., Borsellino C., Pollicino E., Ruisi V. F. (2010): *Experimental and numerical study of composite T-joints for marine application*. International Journal of Adhesion and Adhesives, Vol. 30(5), 347–358.

3. Bigaud J., Aboura Z., Martins A. T., Verger S. (2017): *Analysis of the mechanical behavior of composite T-joints reinforced by one side stitching*. Composite Structures, Vol. 184, 249–255.

4. Blake J. I. R., Shenoi R. A., House J., Turton T. (2001): *Progressive damage analysis of tee joints with viscoelastic inserts*. Composites: Part A, Vol. 32, 641–653.

5. Dharmawan F., Li H. C. H., Herszberg I., John S. (2008): *Applicability of the crack tip element analysis for damage prediction of composite t-joints*. Composite Structures, Vol. 86(1-3), 61–68.

6. Dharmawan F., Thomson R. S., Li H., Herszberg I., Gellert E. (2004): *Geometry and damage effects in a composite marine T-joint*. Composite Structures, Vol. 66,(1-4), 181–187.

7. 7Diler E. A., Özes C., Neser G. (2009): *Effect of T-joint geometry on the performance of a GRP/PVC sandwich system subjected to tension*. Journal of Reinforced Plastics and Composites, Vol. 28, 49.

8. Hellbratt S. E. (1997): *Use of lightweight sandwich joints in a 72m high speed vessel entirely built of carbon fibres*. Composites and Sandwich Structures, 2nd North European Conference (NESCO II), Stockholm, EMAS Publishing, pp. 151–155.

9. Higgins A. (2000): *Adhesive bonding of aircraft structures*. International Journal of Adhesion and Adhesives, Vol. 20(5), 367–376.

10. Huang Z. C., Chen W. D. (2013): *Development of composite connection techniques*. Journal of East China Jiaotong University, Vol. 30(4), 16–29.

11. Khalili S. M. R., Ghaznavi A. (2011): *Numerical analysis of adhesively bonded T-joints with structural sandwiches and study of design parameters*. International Journal of Adhesion & Adhesives, Vol. 31, 347–356.

12. Kumari S., Sinha P. K. (2002): *Finite element analysis of composite wing T-joints*. Journal of Reinforced Plastics & Composites, Vol. 21(17), 1561–1585.

13. Li X. W. (2015): *Design and optimization of composite joints for ship superstructures*. Harbin Engineering University.

14. Padhi G. S., Shenoi R. A., Moy S. S. J., et al. (1998): *Progressive failure and ultimate collapse of laminated composite plates in bending*. Composite Structures, Vol. 40(3), 277–291.

15. Rispler A. R., Steven G. P., Tong L. (1997): *Failure analysis of composite t-joints including inserts*. Journal of Reinforced Plastics & Composites, Vol. 16(18), 1642–1658.

16. Shenoi R. A., Hawkins G. L. (1992): *Influence of material and geometry variations on the behavior of bonded tee connections in FRP ships*. Composites, Vol. 23, 335–345.

17. Shenoi R. A., Read, P. J. C. L., & Hawkins G. L. (1995): *Fatigue failure mechanisms in fibre-reinforced plastic laminated tee joints*. International Journal of Fatigue, Vol. 17(6), 415–426.

18. Shenoi R. A, Violette F. L. M. (1990): *A study of structural composite Tee joints in small boats*. Journal of Composite Materials, Vol. 24(6), 644–66.

19. Shi J., Huang Z. (2012): *Application of composite material in the marine structures*. Fiber Reinforced Plastics / Composites, S1, 269–273.

20. Stickler P. B., Ramulu M. (2001): *Investigation of mechanical behavior of transverse stitched T-joints with PR 520 resin in flexure and tension*. Composite Structures, Vol. 52(3), 307–314.

21. Toftegaard H., Lystrup A. (2005): *Design and test of lightweight sandwich T-joint for naval ships*. Composites Part A, Vol. 36(8), 1055–1065.

22. Van Aanhold J. E., Groves A., Lystrup A., McGeorge D. (2002): *Dynamic and static performance of composite T-joint.* Symposium on Combat Survivability of Air, Space, Sea and Land Vehicles. Denmark: NATO/RTO Aalborg, 1–13.

23. Zhan X. H., Gu C., Wu H. L., Liu H. B., Chen J. C., Chen J., Wei Y. H. (2016): *Experimental and numerical analysis on the strength of 2060 Al-Li alloy adhesively bonded T joints*. International Journal of Adhesion and Adhesives, Vol. 65, 79–87.

CONTACT WITH THE AUTHORS

Xiaowen Li
e-mail: lixw2016@jmu.edu.cn
Jimei University, School of Marine Engineering
Shigu Road, No.176, 361021 Xiamen
China

Zhaoyi Zhu
e-mail: 1988zhuzhaoyi@163.com
Jimei University
Shigu Road, No.176, 361021 Xiamen
China

Yan Li
e-mail: liyan_tju@163.com
Jimei University
Shigu Road, No.176, 361021 Xiamen
China

Zhe Hu
e-mail: huzheok@126.com
Jimei University
Shigu Road, No.176, 361021 Xiamen
China